Accepted Manuscript

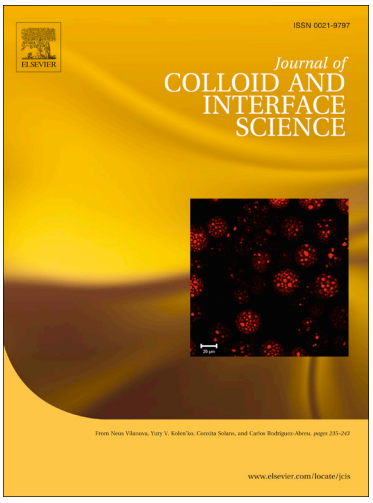

Impact of nanoparticles on the CO_2-brine interfacial tension at high pressure and temperature

Sarmad Al-Anssari, Ahmed Barifcani, Alireza Keshavarz, Stefan Iglauer

PII: S0021-9797(18)30879-8
DOI: https://doi.org/10.1016/j.jcis.2018.07.115
Reference: YJCIS 23906

To appear in: *Journal of Colloid and Interface Science*

Received Date: 6 June 2018
Revised Date: 26 July 2018
Accepted Date: 26 July 2018

Please cite this article as: S. Al-Anssari, A. Barifcani, A. Keshavarz, S. Iglauer, Impact of nanoparticles on the CO_2-brine interfacial tension at high pressure and temperature, *Journal of Colloid and Interface Science* (2018), doi: https://doi.org/10.1016/j.jcis.2018.07.115

Impact of nanoparticles on the CO_2-brine interfacial tension at high pressure and temperature

Sarmad Al-Anssari[1, 2, 3*], Ahmed Barifcani[1], Alireza Keshavarz[3], Stefan Iglauer[3]

[1]*Department of Chemical Engineering, Curtin University, Perth, Australia*

[2]*Department of Chemical Engineering, College of Engineering, University of Baghdad, Iraq*

[3]*School of Engineering, Edith Cowan University, Jundloop, Australia*

[*] Corresponding author

Abstract

Hypothesis: Nanofluid flooding has been identified as a promising method for enhanced oil recovery (EOR) and improved Carbon geo-sequestration (CGS). However, it is unclear how nanoparticles (NPs) influence the CO_2-brine interfacial tension (γ), which is a key parameter in pore-to reservoirs-scale fluid dynamics, and consequently project success. The effects of pressure, temperature, salinity, and NPs concentration on CO_2-silica (hydrophilic or hydrophobic) nanofluid γ was thus systematically investigated to understand the influence of nanofluid flooding on CO_2 geo-storage.

Experiments: Pendant drop method was used to measure CO_2/nanofluid γ at carbon storage conditions using high pressure-high temperature optical cell.

Findings: CO_2/nanofluid γ was increased with temperature and decreased with increased pressure which is consistent with CO_2/water γ. The hydrophilicity of NPs was the major factor; hydrophobic silica NPs significantly reduced γ at all investigated pressures and temperatures while hydrophilic NPs showed only minor influence on γ. Further, increased salinity which increased γ can also eliminate the influence of NPs on CO_2/nanofluid γ. Hence, CO_2/brine γ has low, but, reasonable values (higher than 20 mN/m) at carbon storage conditions even with the presence of hydrophilic NPs, therefore, CO_2 storage can be considered in oil reservoirs after flooding with hydrophilic nanofluid.

The findings of this study provide new insights into nanofluids applications for enhanced oil recovery and carbon geosequestration projects.

Keywords: Nanofluids, Pressure, Temperature, Salinity, Interfacial tension.

1. Introduction

The potential of nanofluids in the upstream oil and gas industry has been highlighted recently [1]; this includes the development of novel nanofluids for enhanced oil recovery (EOR) [2-5], gas recovery [6, 7], drilling [8], fines migration control [9, 10], and fluid flow behavior in the porous medium [11], and, more recently, carbon capture and storage (CCS) projects [12, 13].

In this context of CCS, on which we focus here, there is, however, a serious lack of data and fundamental understanding of CO_2-brine interfacial tension (γ), which is a key parameter determining storage capacity and containment security. For instance, structural and residual trapping are controlled by the capillary pressure (P_c) which is a function of CO_2-water γ and contact angle (θ) between CO_2, water, and the solid surface [14-21].

For an ideal cylindrical capillary tube.

$$P_c = P_{CO_2} - P_{water} = \frac{2\gamma COS(\theta)}{r} \quad (1)$$

where r is the average pore throat radius of the largest connected pore, P_{CO_2} is the pressure in the CO_2 phase, and P_{water} is the pressure in the water phase.

Furthermore, it is well known that P_c determine the pore-scale fluid displacement (e.g. Soll, Celia and Wilson [22]; ØRen and Bakke [23]), which significantly influences the migration of CO_2 plume through the reservoir [24-28], and reservoir-scale fluid dynamics generally [29-31].

The CO_2/water system, particularly at carbon storage conditions, is a complex system. Numerous studies have investigated the effect of pressure, temperature, and salinity on γ of the CO_2/brine system, thus showing that γ decreases with pressure, and slightly increase with temperature and/or salinity [32-37]. However, no data is available for CO_2/nanofluid system despite the fact that nanofluids can in principle enhance CO_2 storage capacities [12, 13].

We, however, note that, Dickson, Binks and Johnston [38] characterized the influence of silica NPs on CO_2 – in – DI-water emulsion stability at room temperature and 22 MPa via

visual observation, turbidity measurements, and optical microscops. Their results revealed that silica NPs can stabilize CO_2/water emulsions, while Roustaei and Bagherzadeh [39] showed that silica NPs slightly increased γ for brine/crude oil system with increasing NPs concentrations at ambient conditions (reaching a plateau at around 0.15 wt% NPs). More recently, Al-Anssari, Wang, Barifcani and Iglauer [40] examined the effect of silica NPs on oil (decane)/brine, and air/brine interfacial tensions at ambient pressure and elevated temperature. Here, a limited effect of NPs on the air/water and oil/water γ was observed, although a combination of NPs with anionic surfactants led to a drastic reduction in γ. Despite these efforts, there is a serious lack of data for of CO_2-aqueous nanofluid γ at carbon storage conditions, which are however key parameters and significantly increase project risk [21]

We thus measured γ of the CO_2-nanofluid system at various pressures, salinities, temperatures, NP concentration and NP hydrophilicity. The results are subsequently discussed in the context of how nanofluid-CO2 γ impacts on CCS storage capacities and containment security.

2. Experimental Methodology

2.1 Material

Hydrophilic silicon dioxide (SiO_2) NPs, purchased from Sigma Aldrich, (particle size: 5-10 nm, and surface area: 140 $m^2.g^{-1}$) were used directly (bare) or after surface modification as hydrophobic (hybrid) NPs. 3-aminopropyl triethoxysilane ($H_2N(CH_2)_3Si(OC_2H_5)_3$ from Sigma Aldrich; mol wt = 221.37 g/mol, Fig.1) was used as a surface modification agent to render the hydrophilicity of NPs (see section 2.2 below), [41, 42]. CO_2 (99.9 mol% from BOC, gas code-082) was used as a supercritical fluid. Deionised (DI)-water (from David Gray; electrical conductivity = 0.02 $mS.cm^{-1}$) and sodium chloride (NaCl; $\geq$ 99.5 mol% purity, from Scharlan) based brine were used as base-fluids to formulate different nanofluids. Potassium chloride (KCl; $\geq$ 99.0 mol% purity) and calcium chloride ($CaCl_2$; $\geq$ 97% purity) purchased from Sigma Aldrich were also used to formulate different brines.

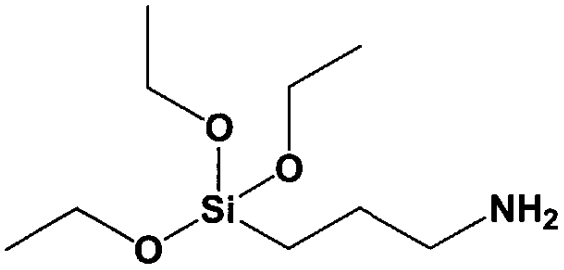

Fig. 1. Chemical structure of (3-aminopropyl) triethoxysilane

2.2 Surface chemistry modification silica NPs

Hydrophilicity of NPs is a key factor for the distribution of nanostructures onto fluid/fluid and solid/fluid interfaces. Thus, the effect of NPs hydrophilicity was investigated. To achieve this, the surface of the original silica NP was modified with 3-aminopropyl triethoxysilane, [41, 42]).

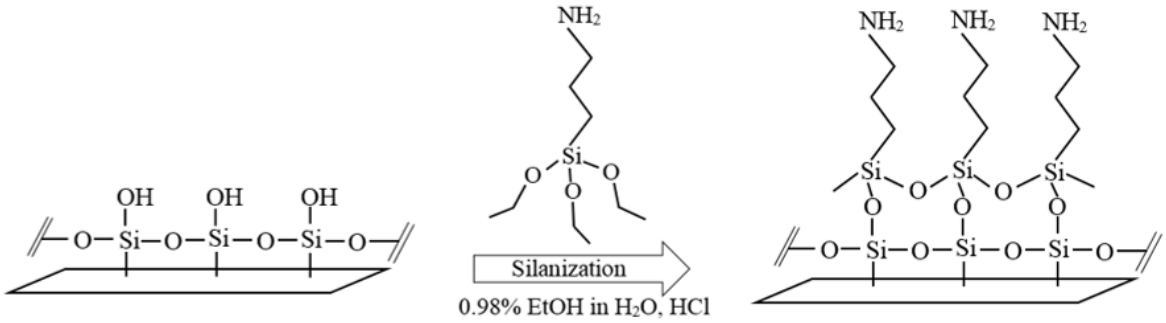

Scheme 1. Attachment of (3-aminopropyl) triethoxysilane to silica nanoparticle surfaces.

Experimentally, 1 g of bare silica NPs were sonicated in 50 mL ethanol using an ultrasonic homogenizer (300 VT Ultrasonic Homogenizer/ BIOLOGICS) for 5 min to prepare a nanoparticle dispersion. In addition, a pre-hydrolyzed solution was prepared by adding 0.7336 g (3-aminopropyl) triethoxysilane into a mixture of 14.82 mL ethanol and 0.18 g water. Note that the amounts of silane, ethanol, and water used depend on the mole number of hydroxyl group existing in 1 g of SiO_2 NPs [43, 44]; thus three molecules of

water are needed for a total hydrolysis of each (3-aminopropyl) triethoxysilane molecule [45]. The pH of the modification solution was kept below the isoelectric point of silica NPs at around 1 – 2 [46] by adding a small amount of concentrated aqueous hydrochloric acid [42]. The modification solution was stirred magnetically for 20 min and then pipetted to the NP dispersion, and the whole mixture was rigorously agitated with a magnetic stirrer for another 24 h, all preparation was done at room conditions. Eventually, silanized NPs were centrifuged and impregnated with ethanol for 24 h to remove the excess silane, then dried at 70°C for 24 h.

2.3 Nanofluids formulation

Nanofluids were formulated via sonication of the insoluble silica NPs in the base fluid using an ultrasonic homogenizer [39, 40]. Different weights of dry hydrophilic or hydrophobic SiO_2 NPs (0.2, 0.4, 1.0, 1.4, 2.0 g) were mixed with 20 ml of different brines (0 – 5 wt% NaCl, KCl, or $CaCl_2$) to formulate nanofluids with different NP concentrations (0.01, 0.02, 0.05, 0.07, 0.10 wt% SiO_2). Each formulation was rigorously dispersed with a 240 W sonication power for 2 min to achieve adequate homogeneity. Note that once dry NPs come into contact with water, the high surface energy NPs tend to aggregate with each other. Efficient sonication is the only way to break down these aggregates and disperse individual NPs in the base fluid. Further, to mimic real CO_2 storage conditions, CO_2 and nanofluid were mixed in a mixing reactor. In this context, nanofluid was stirred with CO_2 in the mixer at the prescribed pressure and temperature for each experiment for 1 h. This is sufficient for equilibrationg water and CO_2 [47]. In all experiments in this work, the fluids were left in the equilibrator for the same period of 1 h to ensure the consistency in all experiments.

2.4 CO_2-nanofluid interfacial tension (γ) measurements

The pendant drop method [48] was used to measure CO_2-nanofluid γ. To achieve this, a high-pressure high-temperature goniometer was used (Fig.2). Initially, the pressure cell was heated to the prescribed temperature, and CO_2 gas was continuously flushed through the cell at ambient pressure for 15 min. Then the outlet valve was closed and further CO_2

was injected into the cell with a high precision syringe pump (ISCO pump model 500D) to raise the pressure to the prescribed value. Once the pressure was stabilized, using a second syringe pump (ISCO pump model 260D), the nanofluid was injected into the cell through a dispensing needle. The second pump was set to a relatively low flow rate (0.4 ml/min) and a drop of nanofluid was produced at the end of the dispensing needle which gradually increased in volume to the point when it fell down due to gravity. A microscopic video camera (Basler scA 640–70 fm, pixel size = 7.4 μm; frame rate = 71 fps; Fujinon CCTV lens: HF35HA-1B; 1:1.6/35 mm) was used to monitor and record the entire process. For γ measurements, images were extracted from the movies files at the instant just before the droplet fell down.

The axisymmetric drop shape analysis (ADSA) was used to digitally measure γ [48-50]. The average standard deviation of γ measurements was ± 2 mN based on replicated measurements (each test was repeated four times).

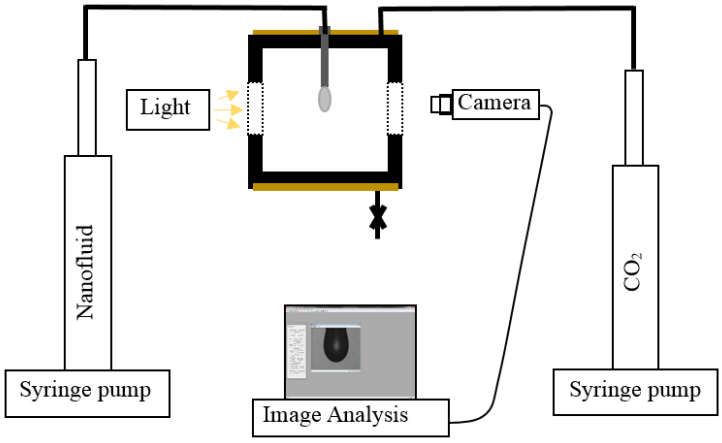

Fig.2. Schematic diagram for interfacial tension (γ) measurement at CO_2 storage condition.

3. Results and Discussion

Despite many studies which have reported the interfacial tension of CO_2-water systems [32-34, 36, 37, 51, 52], no data is available for CO_2/nanofluid systems. Thus here γ of the CO_2/nanofluid system was measured as a function of pressure, temperature, salinity, and

NP load and initial hydrophilicity, to build up the database and to understand the interaction properties of CO_2/ nanofluid systems. The results are discussed in the subsequent sections and related to their potential impact on CCS projects.

3.1 Effect of pressure and temperature on IFT

Initially, to benchmark the measurements against literature data and to gain a baseline for assessment of NP effects, γ of the CO_2/DI-water system was measured at different temperatures (296 K, 313 K, 323 K and 343 K) and pressures (0.1 MPa, 1 MPa, 5 MPa, 15 MPa, and 20 MPa), Fig. 3.

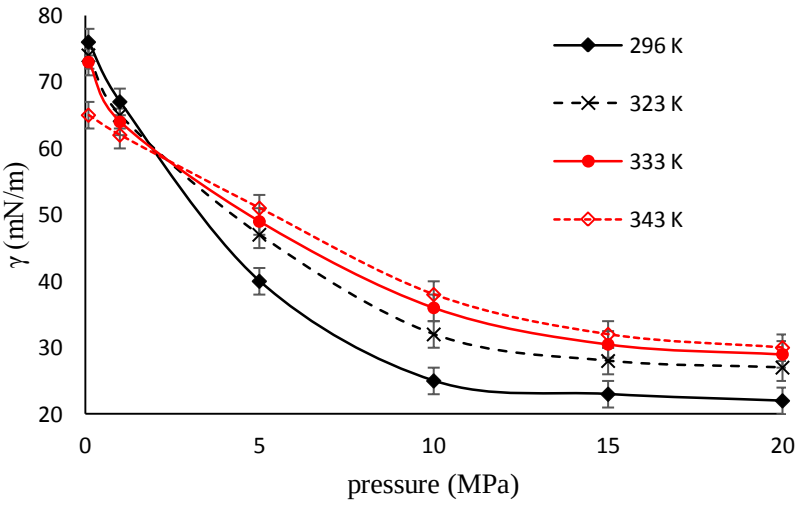

Fig.3. CO_2/DI-water γ as a function of pressure and temperature.

Clearly, at a constant temperature, CO_2-water γ strongly decreased with increasing pressure before reaching almost a pseudo-plateau at around 12 MPa. This is consistent with the reported data in the literature [32-37]. Mechanistically, increased CO_2-pressure increases the anisotropic time-averaged van der Waals attraction for water molecules towards the CO_2 interface [53, 54], thus increasing temperature - which lowers this attraction - increased γ (mN/m), which is consistent with the experimental and published data [34, 36, 51, 55].

3.2 *Effect NP's concentration on γ*

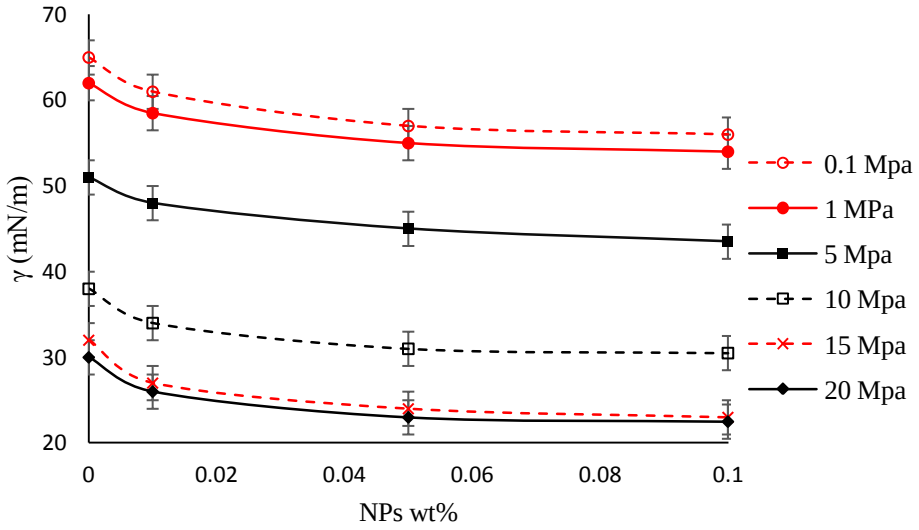

Fig.4. γ of CO_2-nanofluid as a function of NP concentration (0 – 0.1 wt% bare silica NPs in DI-water) at a different pressure (0 – 20 MPa) and constant temperature (343 K).

γ decreased significantly with increasing NP concentrations, Figure 4. For instance, an increase, in NP load from 0 to 0.05 wt% reduced γ by 10% at ambient pressure, and by 12% at 20 MPa (at 343 K). However, further increase in NP concentration (i.e. ≥ 0.05 wt%) showed no more γ reduction. Mechanistically, NPs are adsorbed at the CO_2/water interface, resulting in γ reduction. Thus increased NPs concentration reduced γ until interfacial adsorption capacity was reached [2, 7, 40]. Reaching the adsorption capacity at the fluid/fluid interface prevents further adsorption of NPs onto the interface. Consequently, there is a maximum NP concentration above which γ is no further affected. Note that γ was again influenced by pressure due to above-stated reason.

3.3 *Effect of salt type and concentration on γ*

The effect of salinity on CO_2/nanofluid γ is due to both CO_2 solubility [25] and NPs stability [56]. Considering the fact that salinity and brine chemistry vary widely in subsurface formations [57], the influence of salt type and concentration on CO_2/nanofluid γ was systematically investigated at carbon storage conditions (e.g. 20 MPa and 343 K).

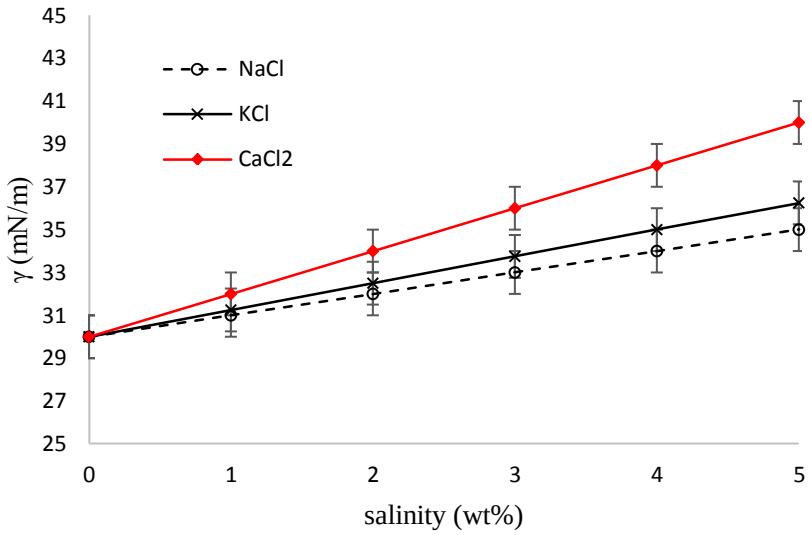

Fig. 5. CO_2/nanofluid (0.01 wt% NPs) γ as a function of the salt type and concentration at high pressure (20 MPa) and Temperature (343 K).

Interfacial tension (γ) increased with salinity following a linear trend. The divalent ion (Ca^{+2}) increased γ significantly which reflects the decreasing in CO_2 solubility in the aqueous phase, consistent with literature data [35]. Monovalent ions (Na^{+}, and K^{+}) showed less effect on CO_2/nanofluid γ, consistent with the reported data concerning CO_2/brine systems [26]. Typically, ion interaction with the uppermost layer of water dominates the effect of salinity on γ. This interaction depends, strongly, on the polarization properties of ions [58]. Mechanistically, ions that being barred from CO_2 phase have an adverse affinity for the interface and are tightly constrained into the bulk of the aqueous phase. Consequently, a significant gradient in ionic strength around the interface is established leading to an amplified attraction of the water molecules into the bulk of the aqueous phase. This leads to increase the required energy for expanding the interfacial area and thus increasing IFT. This phenomenon is expected to be more extensive at both higher ion concentration and ion charge.

3.4 Mutual effect of salts and NPs on IFT at high pressure and temperature

It is well-established that salts have a dramatic impact on NP behavior in the liquid phase [59]. This is due to the screening effect of electrolytes on NP's surface charge and thus

the repulsive forces between NPs [56]. We therefore systematically investigated the mutual effect of salt and NPs on γ (Fig. 6).

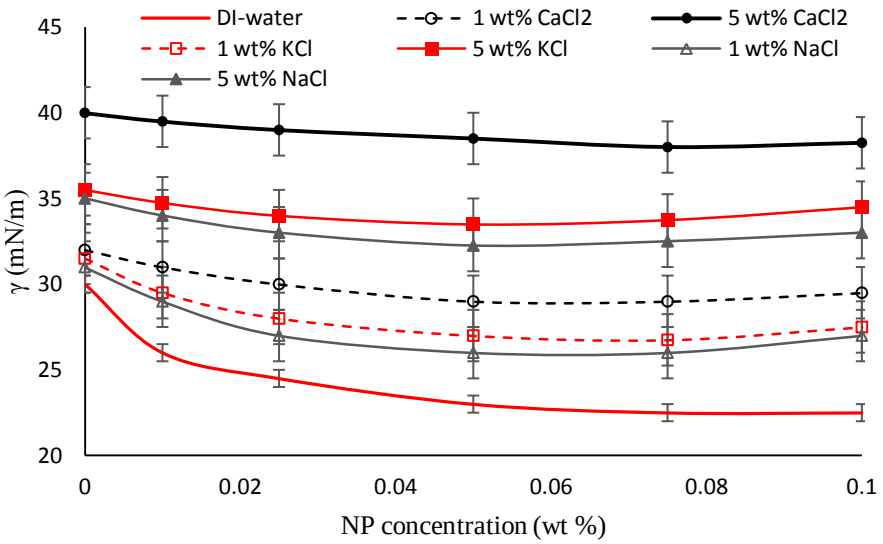

Fig. 6. Mutual effect of various concentrations of NPs and different salts on the IFT of CO_2/brine system at high pressure (20 MPa) and temperature (343 K).

Our results show that salts, particularly at higher concentrations (5wt %), can eliminate the influence of NP on γ. This was true for all ions types, but more significant for the divalent salt ($CaCl_2$). Electrostatic interactions between NPs themselves and the bulk fluid phases determine the NP's effect on the interfacial properties. Furthermore, NPs' surface charges can dramatically change if electrolytes are present, even at very low concentrations [56, 59] which impacts on the adsorption properties of the NPs onto the CO_2/brine interface. In DI-water, the repulsive forces between NPs are sufficient to keep these NPs separated, and they freely move to the CO_2/water interface due to the Brownian motion. However, in brine, the screening effect of the electrolytes on NPs' surface charges can increase the electrostatic van der Waals attraction between NPs leading to accelerated adhesion between the NPs [6]. Further, the resultant larger aggregates will be trapped in the bulk fluid, away from the interface [7]. Thus, less NP influence is noticed in the presence of electrolytes, particularly at higher concentrations.

3.5 *Effect NP's hydrophilicity on γ*

The impact of hydrophilic versus hydrophobic silica NPs on γ was probed, also as a function of their concentration at carbon storage condition, i.e. 20 MPa, and 343 K.

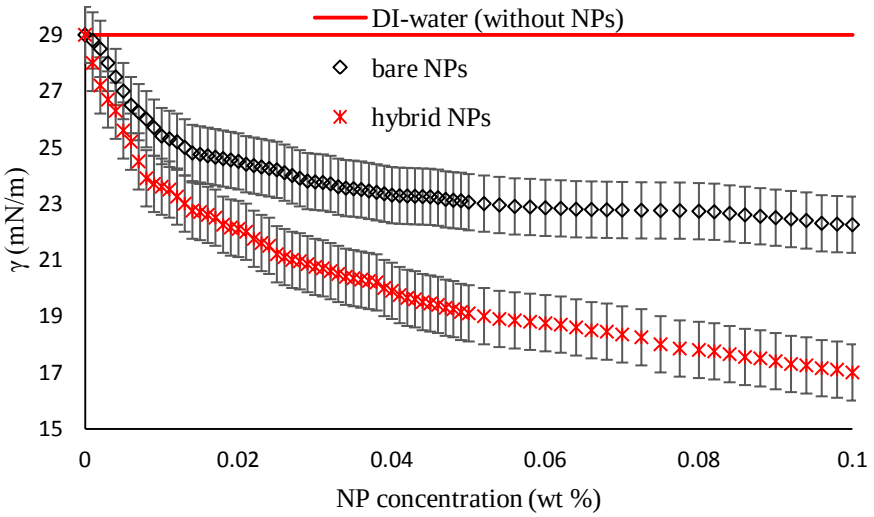

Fig. 7. Effect of NP's concentration and hydrophilicity on CO_2/nanofluids γ 20 at 20 MPa and 343 K.

Clearly, for all NP's concentrations, hydrophobic (hybrid) NPs reduced γ more significantly than the corresponding hydrophilic NPs. Furthermore, γ decreased with increasing NP concentration reaching a pseudo-plateau at around 0.03 wt% for bare NPs, while increasing concentration of hydrophobic NPs continuously reduced γ over the tested concentration range (0 – 0.1wt %). Typically, IFT of pure liquids and fluids is certainly influenced by impurities including all surface active materials such as surfactants and NPs. Mechanistically, when NPs are dispersed in the water phase, they either orientate in the bulk of fluid or travel to the interface depending on the surface properties of the NPs.

This is due to the fact that hydrophilic NPs are tightly packed in the bulk water phase [7], while hydrophobic NPs instantaneously move towards CO_2/water interface (Fig. 8), leading to a more significant γ reduction.

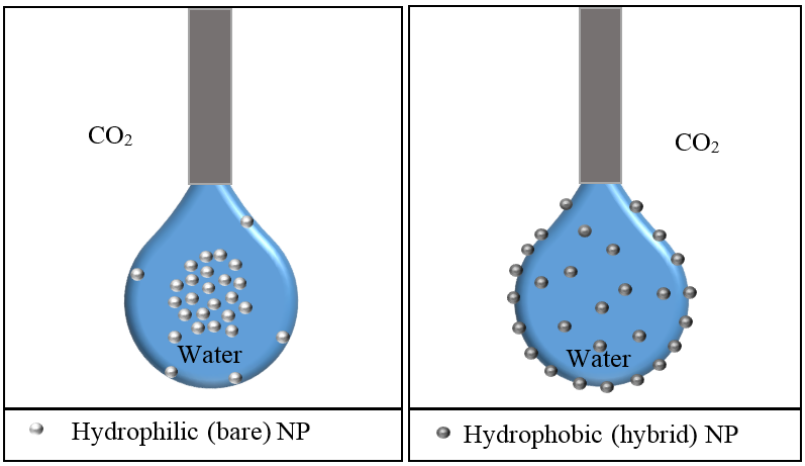

Fig. 8. Interfacial behavior of hydrophilic and hydrophobic nanoparticles in the CO_2/water system.

3.6 NPs adsorption mechanism at the CO_2/water interface

The adsorption/ desorption of NPs at the interface is a complicated phenomenon which mainly attributes to the Brownian motion and the van der Waals energy of the NPs. Typically, mobilization of NPs in the bulk fluid in all directions (i.e. to or away from the interface) is entirely related to the NP's Brownian motion which is resulted from the high surface to volume ratio of nano-sized materials. While the attachment of NPs on the interface and interactions between adjusted particles are controlled by the van der Waals energy. Further, the irreversibility of NPs adsorption is related to the large hydrodynamic forces (weak attraction forces) and the high diffusion coefficient (dispersibility in the solution). Consequently, attachment of NPs on the interface is limited by either the energy barrier which has to be overcome by the particles to attach or detach at the surface or the ability of NPs to diffuse across dispersion media. Thus, the unique feature of the NPs adsorption and desorption phenomena is due to the presence of weak attractive energies which can be overcome by diffusion to facilitate the migration of NPs across different phases.

4. Conclusions

Nanoparticles (NPs) can dramatically influence the interfacial properties of fluid/fluid systems [2, 40]. Such interfacial properties play an important role in fluid flow in porous media [4]. This includes the CO_2-brine interfacial tension (γ) on which we focus here – and which determines CO_2 storage capacity, CO_2 migration in subsurface formations and CO_2 containment security [15, 16, 21, 24, 25, 27, 28, 34, 54]. This study has thus systematically examined the effect of different silica nanoparticles (NPs), inclusion hydrophilic (bare) and hydrophobic (hybrid) NPs on γ at carbon geo-storage conditions (i.e. high pressure and high temperature). The measured data for CO_2-water system (without NPs) were consistent with the reported data in the literature [32-37] in terms of the effect of pressure, temperature, and salinity. The addition of NPs, however, significantly reduced γ. A key factor here is the hydrophilicity of the NPs. Thus an increase in hydrophilic NP concentration (from 0 to 0.05 wt%) reduced γ by 10% at ambient pressure and 12% at 20 MPs, and γ pseudo-plateaued out at ≈ 0.03 wt% NP concentration, consistent with data for oil/nanofluid systems [39, 40]. However, hydrophobic (hybrid) NPs continuously decreased γ with increased hybrid NPs load for all tested concentrations (0 – 0.1 wt% hybrid NPs), by 41 % from 29 to 17 mN/m ±2 at 20 MPs and 343 K, thus hybrid NPs are generally more effective in reducing γ. Furthermore, salts and particularly divalent salts ($CaCl_2$) compensated the effect of NPs on γ. This work thus provides the first insight into the effect of NPs on CO_2-brine interfacial tension (γ) and their potential effects on underground carbon storage projects.

References

[1] L.N. Nwidee, A. Barifcani, M. Lebedev, M. Sarmadivaleh, S. Iglauer, A Realistic Look at Nanostructured Material as an Innovative Approach for Enhanced Oil Recovery Process Upgrading, Recent Insights in Petroleum Science and Engineering, InTech2018.

[2] M. Zargartalebi, N. Barati, R. Kharrat, Influences of hydrophilic and hydrophobic silica nanoparticles on anionic surfactant properties: Interfacial and adsorption behaviors, Journal of Petroleum Science and Engineering 119 (2014) 36-43.

[3] S. Al-Anssari, A. Barifcani, S. Wang, M. Lebedev, S. Iglauer, Wettability alteration of oil-wet carbonate by silica nanofluid, Journal of Colloid and Interface Science 461 (2016) 435-442.

[4] H. Zhang, T.S. Ramakrishnan, A. Nikolov, D. Wasan, Enhanced Oil Recovery Driven by Nanofilm Structural Disjoining Pressure: Flooding Experiments and Microvisualization, Energy & Fuels 30(4) (2016) 2771-2779.

[5] S. Al-Anssari, M. Arif, S. wang, A. Barifcani, L. Maxim, S. Iglauer, Wettability of nanofluid-modified oil-wet calcite at reservoir conditions, Fuel 211 (2018) 405-414.

[6] C. Metin, L. Lake, C. Miranda, Q. Nguyen, Stability of aqueous silica nanoparticle dispersions, Journal of Nanoparticle Research 13(2) (2011) 839-850.

[7] C. Metin, R.T. Bonnecaze, L.W. Lake, C.R. Miranda, Q.P. Nguyen, Aggregation kinetics and shear rheology of aqueous silica suspensions, Applied Nanoscience 4(2) (2012) 169-178.

[8] S. Ponmani, R. Nagarajan, J.S. Sangwai, Effect of Nanofluids of CuO and ZnO in Polyethylene Glycol and Polyvinylpyrrolidone on the Thermal, Electrical, and Filtration-Loss Properties of Water-Based Drilling Fluids, SPE Journal 21(2) (2015) 405-415.

[9] A. Habibi, M. Ahmadi, P. Pourafshary, s. Ayatollahi, Y. Al-Wahaibi, Reduction of Fines Migration by Nanofluids Injection: An Experimental Study, (2012).

[10] X. Zheng, F. Perreault, J. Jang, Fines adsorption on nanoparticle-coated surface, Acta Geotechnica 13(1) (2018) 219-226.

[11] N. Solovitch, J. Labille, J. Rose, P. Chaurand, D. Borschneck, M.R. Wiesner, J.-Y. Bottero, Concurrent Aggregation and Deposition of TiO_2 Nanoparticles in a Sandy Porous Media, Environmental Science & Technology 44(13) (2010) 4897-4902.

[12] S. Al-Anssari, M. Arif, S. Wang, A. Barifcani, M. Lebedev, S. Iglauer, CO_2 geo-storage capacity enhancement via nanofluid priming, International Journal of Greenhouse Gas Control 63 (2017) 20-25.

[13] S. Al-Anssari, M. Arif, S. Wang, A. Barifcani, M. Lebedev, S. Iglauer, Wettability of nano-treated calcite/CO_2/brine systems: Implication for enhanced CO_2 storage potential, International Journal of Greenhouse Gas Control 66 (2017) 97-105.

[14] K. Chaudhary, M. Bayani Cardenas, W.W. Wolfe, J.A. Maisano, R.A. Ketcham, P.C. Bennett, Pore-scale trapping of supercritical CO_2 and the role of grain wettability and shape, Geophysical Research Letters 40(15) (2013) 3878-3882.

[15] S. Iglauer, A.Z. Al-Yaseri, R. Rezaee, M. Lebedev, CO_2 wettability of caprocks: Implications for structural storage capacity and containment security, Geophysical Research Letters 42(21) (2015) 9279-9284.

[16] S. Iglauer, C.H. Pentland, A. Busch, CO_2 wettability of seal and reservoir rocks and the implications for carbon geo-sequestration, Water Resources Research 51(1) (2015) 729-774.

[17] A.S. Al-Menhali, S. Krevor, Capillary Trapping of CO_2 in Oil Reservoirs: Observations in a Mixed-Wet Carbonate Rock, Environmental Science & Technology 50(5) (2016) 2727-2734.

[18] A.S. Al-Menhali, H.P. Menke, M.J. Blunt, S.C. Krevor, Pore Scale Observations of Trapped CO_2 in Mixed-Wet Carbonate Rock: Applications to Storage in Oil Fields, Environmental Science & Technology 50(18) (2016) 10282-10290.

[19] T. Rahman, M. Lebedev, A. Barifcani, S. Iglauer, Residual trapping of supercritical CO_2 in oil-wet sandstone, Journal of Colloid and Interface Science 469 (2016) 63-68.

[20] M. Arif, F. Jones, A. Barifcani, S. Iglauer, Electrochemical investigation of the effect of temperature, salinity and salt type on brine/mineral interfacial properties, International Journal of Greenhouse Gas Control 59 (2017) 136-147.

[21] S. Iglauer, CO_2–Water–Rock Wettability: Variability, Influencing Factors, and Implications for CO_2 Geostorage, Accounts of Chemical Research (2017).

[22] W. Soll, M. Celia, J. Wilson, Micromodel studies of three-fluid porous media systems: Pore-scale processes relating to capillary pressure-saturation relationships, Water resources research 29(9) (1993) 2963-2974.

[23] P.-E. ØRen, S. Bakke, Process Based Reconstruction of Sandstones and Prediction of Transport Properties, Transp Porous Med 46(2) (2002) 311-343.

[24] X. Tianfu, A.J. A., P. Karsten, Reactive geochemical transport simulation to study mineral trapping for CO_2 disposal in deep arenaceous formations, Journal of Geophysical Research: Solid Earth 108(B2) (2003).

[25] P. Chiquet, J.-L. Daridon, D. Broseta, S. Thibeau, CO_2/water interfacial tensions under pressure and temperature conditions of CO_2 geological storage, Energy Conversion and Management 48(3) (2007) 736-744.

[26] S. Bachu, D.B. Bennion, Interfacial Tension between CO_2, Freshwater, and Brine in the Range of Pressure from (2 to 27) MPa, Temperature from (20 to 125) °C, and Water Salinity from (0 to 334 000) mg·L−1, Journal of Chemical & Engineering Data 54(3) (2009) 765-775.

[27] E.A. Al-Khdheeawi, S. Vialle, A. Barifcani, M. Sarmadivaleh, S. Iglauer, Impact of reservoir wettability and heterogeneity on CO_2-plume migration and trapping capacity, International Journal of Greenhouse Gas Control 58 (2017) 142-158.

[28] Al-Khdheeawi, V. Stephanie, B. Ahmed, S. Mohammad, Z. Yihuai, I. Stefan, Impact of salinity on CO_2 containment security in highly heterogeneous reservoirs, Greenhouse Gases: Science and Technology 8(1) (2018) 93-105.

[29] M. Sahimi, Flow and transport in porous media and fractured rock: from classical methods to modern approaches, John Wiley & Sons2011.

[30] J. Bear, Dynamics of fluids in porous media, Courier Corporation2013.

[31] M.J. Blunt, Multiphase flow in permeable media: A pore-scale perspective, Cambridge University Press2017.

[32] K.L. Harrison, Interfacial tension measurements of CO_2-polymer and CO_2-water systems and formation of water-in-CO_2 microemulsions, The University of Texas at Austin, Ann Arbor, 1996, p. 286.

[33] A. Hebach, A. Oberhof, N. Dahmen, A. Kögel, H. Ederer, E. Dinjus, Interfacial Tension at Elevated PressuresMeasurements and Correlations in the Water + Carbon Dioxide System, Journal of Chemical & Engineering Data 47(6) (2002) 1540-1546.

[34] C. Chalbaud, M. Robin, J.M. Lombard, F. Martin, P. Egermann, H. Bertin, Interfacial tension measurements and wettability evaluation for geological CO_2 storage, Advances in Water Resources 32(1) (2009) 98-109.

[35] X. Li, E. Boek, G.C. Maitland, J.P.M. Trusler, Interfacial Tension of (Brines + CO_2): (0.864 NaCl + 0.136 KCl) at Temperatures between (298 and 448) K, Pressures between (2 and 50) MPa, and Total Molalities of (1 to 5) mol·kg–1, Journal of Chemical & Engineering Data 57(4) (2012) 1078-1088.

[36] M. Sarmadivaleh, A.Z. Al-Yaseri, S. Iglauer, Influence of temperature and pressure on quartz–water–CO_2 contact angle and CO_2–water interfacial tension, Journal of Colloid and Interface Science 441(0) (2015) 59-64.

[37] M. Arif, A.Z. Al-Yaseri, A. Barifcani, M. Lebedev, S. Iglauer, Impact of pressure and temperature on CO_2–brine–mica contact angles and CO_2–brine interfacial tension: Implications for carbon geo-sequestration, Journal of Colloid and Interface Science 462 (2016) 208-215.

[38] J.L. Dickson, B.P. Binks, K.P. Johnston, Stabilization of Carbon Dioxide-in-Water Emulsions with Silica Nanoparticles, Langmuir 20(19) (2004) 7976-7983.

[39] A. Roustaei, H. Bagherzadeh, Experimental investigation of SiO_2 nanoparticles on enhanced oil recovery of carbonate reservoirs, J Petrol Explor Prod Technol (2014) 1-7.

[40] S. Al-Anssari, S. Wang, A. Barifcani, S. Iglauer, Oil-water interfacial tensions of silica nanoparticle-surfactant formulations, Tenside Surfactants Detergents 54(4) (2017) 334-341.

[41] J.W. Grate, K.J. Dehoff, M.G. Warner, J.W. Pittman, T.W. Wietsma, C. Zhang, M. Oostrom, Correlation of Oil–Water and Air–Water Contact Angles of Diverse Silanized Surfaces and Relationship to Fluid Interfacial Tensions, Langmuir 28(18) (2012) 7182-7188.

[42] G. London, G.T. Carroll, B.L. Feringa, Silanization of quartz, silicon and mica surfaces with light-driven molecular motors: construction of surface-bound photo-active nanolayers, Organic & Biomolecular Chemistry 11(21) (2013) 3477-3483.

[43] J.-Z. Ma, J. Hu, Z.-J. Zhang, Polyacrylate/silica nanocomposite materials prepared by sol–gel process, European Polymer Journal 43(10) (2007) 4169-4177.

[44] W. He, D. Wu, J. Li, K. Zhang, Y. Xiang, L. Long, S. Qin, J. Yu, Q. Zhang, Surface modification of colloidal silica nanoparticles: Controlling the size and grafting process, Bulletin of the Korean Chemical Society 34(9) (2013) 2747-2752.

[45] P. Rostamzadeh, S.M. Mirabedini, M. Esfandeh, APS-silane modification of silica nanoparticles: effect of treatment's variables on the grafting content and colloidal stability of the nanoparticles, Journal of Coatings Technology and Research 11(4) (2014) 651-660.

[46] Q.A. Bhatti, M.K. Baloch, S. Schwarz, G. Petzold, Effect of Various Parameters on the Stability of Silica Dispersions, Journal of Solution Chemistry 43(11) (2014) 1916-1928.

[47] R.M. El-Maghraby, C.H. Pentland, S. Iglauer, M.J. Blunt, A fast method to equilibrate carbon dioxide with brine at high pressure and elevated temperature including solubility measurements, The Journal of Supercritical Fluids 62 (2012) 55-59.

[48] W. Xing, Y. Song, Y. Zhang, M. Nishio, Y. Zhan, W. Jian, Y. Shen, Research Progress of the Interfacial Tension in Supercritical CO2-water/oil System, Energy Procedia 37 (2013) 6928-6935.

[49] P. Cheng, D. Li, L. Boruvka, Y. Rotenberg, A.W. Neumann, Automation of axisymmetric drop shape analysis for measurements of interfacial tensions and contact angles, Colloids and Surfaces 43(2) (1990) 151-167.

[50] S.M.I. Saad, A.W. Neumann, Axisymmetric Drop Shape Analysis (ADSA): An Outline, Advances in Colloid and Interface Science 238 (2016) 62-87.

[51] A. Georgiadis, G. Maitland, J.P.M. Trusler, A. Bismarck, Interfacial Tension Measurements of the (H_2O + CO_2) System at Elevated Pressures and Temperatures, Journal of Chemical & Engineering Data 55(10) (2010) 4168-4175.

[52] Y. Liu, M. Mutailipu, L. Jiang, J. Zhao, Y. Song, L. Chen, Interfacial tension and contact angle measurements for the evaluation of CO_2-brine two-phase flow characteristics in porous media, Environmental Progress & Sustainable Energy 34(6) (2015) 1756-1762.

[53] J.C. Santamarina, J. Jang, Energy geotechnology: Implications of mixed fluid conditions, 5th International Conference on Unsaturated Soil, Taylor & Francis Group, London, ISBN 978-0-415-60428-4, Bacelona, Spain, 2011, pp. 33-50.

[54] D.N. Espinoza, S.H. Kim, J.C. Santamarina, CO_2 geological storage — Geotechnical implications, KSCE Journal of Civil Engineering 15(4) (2011) 707-719.

[55] M. Arif, A. Barifcani, S. Iglauer, Solid/CO_2 and solid/water interfacial tensions as a function of pressure, temperature, salinity and mineral type: Implications for CO2-wettability and CO_2 geo-storage, International Journal of Greenhouse Gas Control 53 (2016) 263-273.

[56] S. Al-Anssari, M. Arif, S. Wang, A. Barifcani, S. Iglauer, Stabilising nanofluids in saline environments, Journal of Colloid and Interface Science 508 (2017) 222-229.

[57] L.P. Dake, Fundamentals of Reservoir Engineering, Elsevier, 1978.

[58] K. Johansson, J.C. Eriksson, γ and dγ/dT measurements on aqueous solutions of 1,1-electrolytes, Journal of Colloid and Interface Science 49(3) (1974) 469-480.

[59] A. Amiri, G. Øye, J. Sjöblom, Influence of pH, high salinity and particle concentration on stability and rheological properties of aqueous suspensions of fumed silica, Colloids and Surfaces A: Physicochemical and Engineering Aspects 349(1–3) (2009) 43-54.

Graphical abstract